2008 American Control Conference
Westin Seattle Hotel, Seattle, Washington, USA
June 11-13, 2008



# Motion Planning for a Diesel Oxidation Catalyst Outlet Temperature

Olivier Lepreux, Yann Creff and Nicolas Petit

*Abstract*— **A simple distributed parameter model is proposed for a Diesel Oxidation Catalyst (DOC). This model focuses on the propagation of the inlet temperature variations. The inlet-to-outlet temperature transfer function is computed. Its inversion allows to derive an open-loop control law corresponding to finite-time transitions of the outlet temperature. However, this straightforward strategy has some shortcomings. In particular, the obtained control histories are, for presented cases of engineering interest, inconsistent with the performance of available actuators. To address this issue, a constrained optimization approach is proposed. The results lead to a surprisingly simple control law.**

## I. INTRODUCTION

Over the past decades, automotive emissions standards have steadily become more stringent [1]. In particular, to meet the requirements of particulate matter emission standards, engines have been consequently upgraded. A prime example is the Diesel Particulate Filter (DPF) which is found on most new vehicles.

During regeneration [2], DPFs behave like potentially unstable reactors [3]. Their inlet temperature must be carefully controlled. In most configurations, a Diesel Oxidation Catalyst (DOC) is located upstream the DPF in the vehicle exhaust line. To increase the DPF inlet temperature, reductants are oxidized in the DOC, which, in turn, increases its outlet temperature. The DOC also conveys, up to some heat losses, its inlet enthalpy flow: in other words, inlet temperature variations propagate through the DOC. In the vast majority of studies found in the literature, the amount of reductants is the control variable, while the DOC inlet temperature can be regarded as a disturbance. However, the release of the reductants reaction enthalpy implies outlet temperature variations, that much resemble those due to inlet temperature variations. Therefore, it seems relevant, in a first attempt, in order to correctly understand how the system works and should be controlled, not to consider any chemical reaction (that would complexify the analysis), and to assume that the inlet temperature can be used as a control variable. Results of this first study could also find applications in the light-off phases [4] (when the catalyst is not hot enough to oxidize the reductants), or for -rarely used- electrically-heated systems [5]. In this context, the problem of motion planning is fundamental. To address this issue, we propose an open-loop control strategy which is based on an inversion of a presented partial differential equation (PDE) model.

Experimentally, it can be observed that a step change on the inlet temperature leads to long response times [4] (a typical order of magnitude is 100 s, while gas flows through the DOC in a fraction of a second). Depending on the engine outlet gas flow rate, these response times significantly vary: they roughly increase by a factor of 10 from idle speed to full load. Control strategies that are usually used to deal with this problem rely on mappings, which, in practice, are difficult (and tedious) to calibrate. We believe that a better understanding of the system behavior can improve the control performances.

In this paper, we present a motion planning technique for the DOC system. A DOC is designed to improve the mass transfer characteristics to the catalytic surface. To this end, the channels of the monolith are narrow and numerous (of the order of 1000). This geometric configuration leads to highly-efficient heat transfer between gas and solid. Hence, the solid phase (i.e. the monolith) acts as a spatially-distributed energy reservoir and this phenomenon leads to highly-delayed temperature responses. We take this fact into account in our control-oriented model. This model is validated experimentally, and then used for motion planning. Its infinite dimensional form is fully accounted for in the control strategy.

The paper is organized as follows. In Section II we formulate the control-oriented model. In Section III we calculate the control by an inversion-based approach. Depending on numerical values, this formal approach may lead to unapplicable results. In Section IV an optimization method is used to generate trajectories under input constraints.

## II. PROBLEM FORMULATION

### A. Balance and Transfer Phenomena Equations

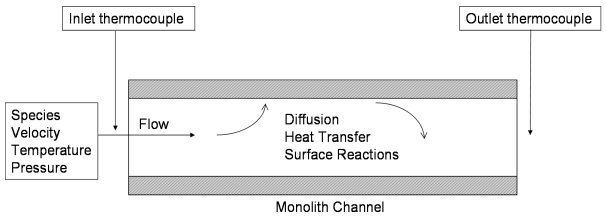


1: Scheme of governing phenomena involved in a DOC

Numerous models have been used and improved since the 1960s for catalysts [6]. Fig. (1) illustrates the main phenomena involved in a DOC. A simple model, leaving

Manuscript received September 18, 2007.

O. Lepreux and Y. Creff are with IFP Lyon, Technology, Computer Science and Applied Mathematics Division, BP 3, 69390 Vernaison, France (email: olivier.lepreux@ifp.fr and yann.creff@ifp.fr)

N. Petit is with the Centre Automatique et Systèmes, École Nationale Supérieure des Mines de Paris, 60, bd. Saint-Michel, 75272 Paris Cedex 06, France (email: nicolas.petit@ensmp.fr)

out chemical reactions, can be written with energy balances for the gas phase (1) and the solid phase (2)

$$\varepsilon\rho_g C_{p,g}\frac{\partial T_g}{\partial t} + \frac{F}{A_{cell}}C_{p,g}\frac{\partial T_g}{\partial z} = \frac{\partial}{\partial z}\left(\varepsilon k_g \frac{\partial T_g}{\partial z}\right) - h_g G_a (T_g - T_s) \quad (1)$$

$$(1-\varepsilon)\rho_s C_{p,s}\frac{\partial T_s}{\partial t} = \frac{\partial}{\partial z}\left((1-\varepsilon)k_s \frac{\partial T_s}{\partial z}\right) + h_g G_a (T_g - T_s) \quad (2)$$

In (1) and (2), the following symbols are used: subscript $g$ (resp. $s$) refers to the gas (resp. the monolith), $T$ is the temperature, $\rho$ is the density, $C_p$ is the constant pressure specific heat, $A_{cell}$ is the Vardi and Biller area of cell [7], $F$ is the mass flow rate, $G_a$ is the geometric surface area-to-volume ratio, $\varepsilon$ is the void fraction and $k$ is the thermal conductivity.

### B. Control-Oriented Model

According to [6] we can make the following simplifying assumptions. Because of the symmetry, heat losses to the surroundings are neglected. Axial diffusion in the fluid phase is negligible since the Peclet number [8] is large Pe>50 while the axial conduction in the solid is not important. Except under very high flow rate conditions, the entry length is a small fraction of the converter length. As a result, the Nusselt and Sherwood numbers [8] can be assumed equal to the fully-developed flow constant values. Rewriting (1) and (2) with the following normalizing parameters

$$\begin{cases} k_1 &= \dfrac{h_g G_a}{\varepsilon\rho_g C p_g} \\ k_2 &= \dfrac{h_g G_a}{(1-\varepsilon)\rho_s C p_s} \\ v &= \dfrac{F}{\varepsilon\rho_g A_{cell}} \\ T &= T_g \end{cases} \quad (3)$$

we obtain the following control-oriented model

$$\begin{cases} \dfrac{\partial T}{\partial t} + v\dfrac{\partial T}{\partial z} &= -k_1(T - T_s) \\ \dfrac{\partial T_s}{\partial t} &= k_2(T - T_s) \end{cases} \quad (4)$$

The variable $v$ represents the speed of the gas flowing through the DOC, and can be easily computed from (3). The set of parameters $(k_1, k_2)$ can either be deduced from usual correlations [8] or identified from experimental step changes in the inlet temperature as detailed in Subsection II-E. We assume that the reactor is initially at steady state, i.e. $T(z,0)$ and $T_s(z,0)$ are equal and constant. It is then correct to assume that $T$ and $T_s$ represent the variations of temperature about steady state instead of the temperatures themselves. Hence we have an infinite-dimensional linear model. The conditions at $t = 0$ are

$$\begin{cases} T(z,0) = 0 \\ T_s(z,0) = 0. \end{cases} \quad (5)$$

The inlet temperature can be considered as the control variable

$$T(0,t) = T_0 \triangleq u(t). \quad (6)$$

The output of the system $y$ is the outlet temperature

$$y(t) = T(L,t)$$

where $L$ is length of the DOC.

### C. Input-Output Response

The formal general response to an input signal can be calculated using operational calculus with respect to the time variable. We denote $\mathcal{L}^{-1}$ the inverse Laplace operator, $\hat{x}$ the Laplace transform of $x$, $s$ the Laplace variable and, $\Upsilon$ the Heaviside function. Equations (4) and (5) lead to

$$\begin{cases} s\hat{T} + v\dfrac{\partial \hat{T}}{\partial z} = -k_1(\hat{T} - \hat{T}_s) \\ s\hat{T}_s = k_2(\hat{T} - \hat{T}_s). \end{cases}$$

The boundary control (6) is transformed into

$$\hat{T}(0,s) = \hat{u}(s).$$

This leads to the following first-order differential equation

$$\frac{\partial \hat{T}}{\partial z} = \frac{1}{v}\left(\frac{-k_1 s}{s+k_2} - s\right)\hat{T}$$

Hence,

$$\hat{T}(z,s) = \hat{u}(s)\exp\left(-\frac{z}{v}s - \frac{k_1 z}{v} + \frac{m}{s+k_2}\right) \quad (7)$$

where $m = k_1 k_2 z/v$. Using inverse Laplace transforms, we get (refer to Appendix VI-A for details)

$$T(z,t) = \Upsilon(t - \frac{z}{v})e^{-\frac{k_1 z}{v}} \times \left[u(t - \frac{z}{v}) + \ldots \right.$$
$$\left. \ldots \int_0^{t-z/v} e^{-k_2\tau}\sqrt{\frac{m}{\tau}} I_1(2\sqrt{m\tau})u(t - \frac{z}{v} - \tau)d\tau\right].$$

### D. Step Response

In particular, the step response is computed for $u(t) = \Upsilon(t)$ and can be written

$$T(z,t) = \Upsilon(t - \frac{z}{v})\exp\left(-\frac{k_1 z}{v}\right)\times \left[1 + \int_0^{t-z/v}\exp\left(-k_2\tau\right)\sqrt{\frac{m}{\tau}} I_1(2\sqrt{m\tau})d\tau\right]. \quad (8)$$

For efficient numeric evaluation of the above expression, we can use the following convergent power series expansion (see Appendix VI-B for calculation details)

$$T(z,t) = \exp\left(-\frac{k_1 z}{v}\right)\Upsilon(t - z/v)\times \left[1 + \sum_{r=1}^{\infty}\frac{\Gamma_{\text{inc}}(k_2(t - z/v), r)}{r!(k_2/m)^r}\right]. \quad (9)$$

Note that the static gain $G$ can be computed using (7) when $u(t) = \Upsilon(t)$. Accordingly to the fact that heat losses have been neglected, we have $G = \lim_{s\to 0} \hat{T}(z,s) = 1$.

### E. Experimental Validation of the Model

Parameters $(k_1, k_2)$ can be easily identified from experiments. Since the model is linear, and the gain of the transfer function is equal to 1, we use normalized temperature for identification. As shown in Fig. (2), the model kindly fits the experimental data.

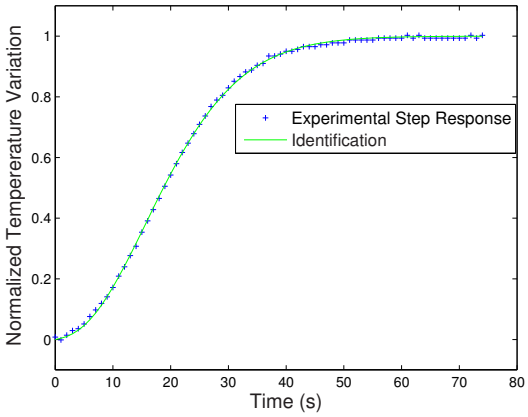


2: Identification to experimental results

## III. INVERSION-BASED OPEN-LOOP CONTROL

To solve the motion planning problem, i.e. to compute control law corresponding to some desired output transients, we propose an open-loop control law based on a formal inversion of the input-output transfer function.

### A. Inverse Control

It is straightforward to invert (7) and formulate $\hat{u}(s)$ as a function of the output $\hat{y}(s)$ for $z = L$

$$\hat{u}(s) = \exp\left(\frac{z}{v}s + \frac{k_1 z}{v} - \frac{m}{s+k_2}\right)\hat{y}(s). \qquad (10)$$

The output $y(t)$ can be any delayed function of time. This delay equals $z/v$. Let $f(t)$ denote this function. We can write

$$\hat{y}(s) = \exp\left(-\frac{z}{v}s\right)\hat{f}(s). \qquad (11)$$

Combining (10) and (11) we get

$$\hat{u}(s) = \exp\left(\frac{k_1 z}{v} - \frac{m}{s+k_2}\right)\hat{f}(s).$$

The inverse Laplace calculus detailed in Appendix VI-C leads to

$$\begin{cases} u(t) = e^{\dfrac{k_1 z}{v}}\,\Upsilon(t)\times \\ \left[f(t) - \displaystyle\int_0^t \sqrt{\frac{m}{\tau}} J_1(2\sqrt{m\tau})\exp\left(-k_2\tau\right) f(t-\tau)d\tau\right] \\ y(t) = f(t - z/v) \end{cases} \qquad (12)$$

In our application, the dead time $z/v$ (typically $10^{-2}$ s) is very small when compared to the response time of the system (typically $10^2$ s), so that $f(t)$ can be almost regarded as $y(t)$.

### B. Simulation Results

In this section we illustrate our results with two realistic scenarios. In case A, we use $k_1 = 400$ s$^{-1}$, $k_2 = 0.35$ s$^{-1}$ and $v = 4$ m.s$^{-1}$. In case B, we use $k_1 = 1600$ s$^{-1}$, $k_2 = 0.82$ s$^{-1}$ and $v = 4.6$ m.s$^{-1}$. These are two different cases corresponding to low air flow rate and long response time, which are in practice the most problematic to control. To obtain all the presented numerical results, we use a catalyst length $L = 7.62$ cm (3 inches). Because the system is linear and the static gain is 1, figures are plotted with normalized temperature responses. The choice of the trajectory is *a priori* free, but several tries of usual transition functions have shown us it has important consequences. In order to obtain a smooth transition we choose the following $C^\infty$ Gevrey function of order $1 + \frac{1}{\gamma}$ (see [9] for the mathematical properties of this function)

$$\begin{cases} f(\frac{t}{t_f}) = 0 \quad \text{if} \quad \frac{t}{t_f} \leq 0 \\ f(\frac{t}{t_f}) = \dfrac{\displaystyle\int_0^{\frac{t}{t_f}} \exp\left(-\left(\frac{1}{u(1-u)}\right)^\gamma\right)du}{\displaystyle\int_0^1 \exp\left(-\left(\frac{1}{u(1-u)}\right)^\gamma\right)du} \quad \text{if } 0 < \frac{t}{t_f} < 1 \\ f(\frac{t}{t_f}) = 1 \quad \text{if} \quad \frac{t}{t_f} \geq 1 \end{cases}$$

Transition times $t_f$ chosen in this section are inspired from results obtained in Section IV. They are realistic. We use $t_f = 21.5$ s for case A and $t_f = 38.5$ s for case B, and $\gamma = 0.6$ for both cases. Depending on the values of parameters $(k_1, k_2, v)$, we can get drastically different types of control trajectories. Although not intuitive, control presented for case A in Fig. (3a) is quite simple. For case B, on the other hand, the control presented in Fig. (3b) is unrealistic because of its frequency and its amplitude. Further, in this case (actually probably in both cases) the control obtained by inversion goes far beyond the model validity region (non negligible conduction, non constants coefficients and non negligible heat losses ...). However, the computed control stresses interesting problems, related to the high-capacity energy storage of the solid phase. This partly explains why a DOC is a difficult system to control.

## IV. TRAJECTORY OPTIMIZATION FOR CONSTRAINED INPUT

As seen in Section III, inversion of the model can lead to a "shaking" control. Actually, this does not mean that such a system cannot be accelerated, but attention must be paid to the control bounds. In this section, to address this issue, we generate output trajectories under input constraints. First, we use a classical optimization approach, then we formulate the problem in a different way: we impose a limited number of possible values for the control, and a limited number of switches between these values. This drastically reduces the number of optimization variables, whereas the loss of performance is negligible.

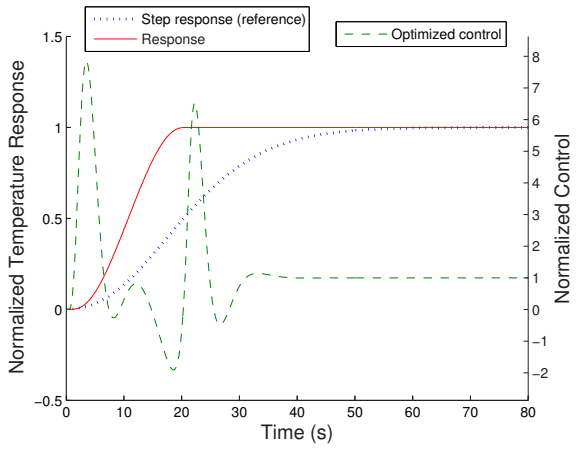


(a) Case A

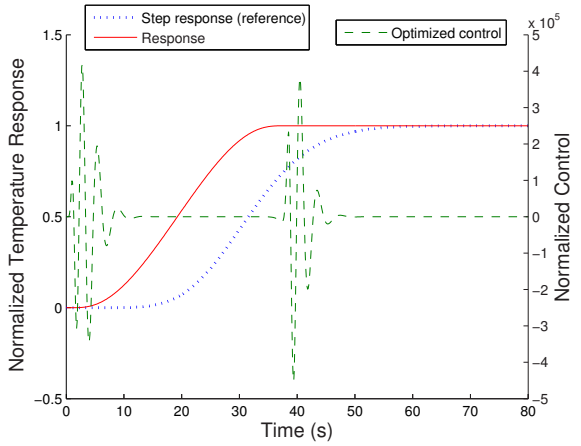


(b) Case B

3: Control corresponding to a smooth finite-time transition

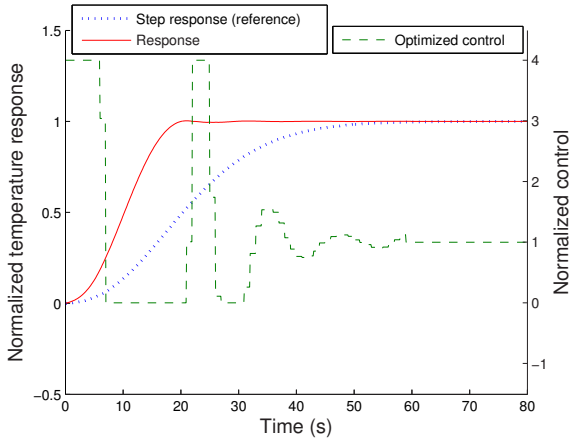


(a) Case A

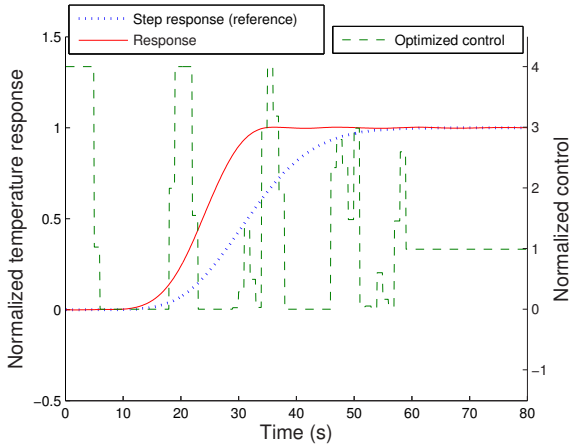


(b) Case B

4: Optimized control with method 1

### A. *Problem Formulation 1 and Simulation Results*

In this first formulation, we want to compute a piecewise constant control, subject to lower and upper bounds. This problem can be formally written under the form

$$\min_{(u_0,\ldots,u_n)} \int_0^H (y^c - y(\tau))^2 d\tau$$

$$\begin{cases} u_{min} \leq u_i = u(iT_u) \leq u_{max} & \forall i \in \{0,\ldots,n\} \\ y(t) \leq y^c + \varepsilon & \forall t \in [0,H] \\ y(t) \geq y^c - \varepsilon & \forall t \in [T,H] \end{cases} \tag{13}$$

where $y^c$ is the setpoint, $\varepsilon$ is a small positive constant, $T_u$ is the control sampling period, $nT_u$ is the control horizon, and $H$ is the prediction horizon. $T$ corresponds to the minimum time for which problem (13) is feasible. It is found iteratively, for example by dichotomy. Enforcing this minimum constraint avoids oscillations after the rise time. For numeric evaluation, we use $y^c = 1$, $n = 60$, $T_u = 1$ s, $H = 200$ s, $u_{min} = 0$, $u_{max} = 4$, and $\varepsilon = 0.003$. As seen in Subsection II-B, the model is linear. Hence, for numerical experiments, its response to a given piecewise constant input can be quickly evaluated by a linear combination of time-delayed step responses. Step response $g$ is evaluated by (9) and $y$ is given by

$$y(t) = u_0\ g(t) + \sum_{i=1}^{n} (u_i - u_{i-1})\ g(t - iT_u)$$

Fig. (4a) and (4b) show that, in both cases, the system is accelerated as in Section III, but, now, input constraints are satisfied. The transitions are not achieved in finite-time but, from the end time used in Section III, the output remains within a tight range around the final value.

### B. *Problem Formulation 2 and Simulation Results*

The second method presented in this subsection allows to further simplify the control with minor consequences on performance. We can notice in Subsection IV-A that the control presents numerous pulses before finally setting to 1. In other words, once the output has almost reached its final value, the control still acts over a long period. We would like to shorten this period for an easier implementation of the control. To this end, we consider only a limited number of pulses $N$, before the final control value is kept constant. The $N$ pulses share the same magnitude (equal to the allowed maximum $u_{max}$), while their switch times have to be

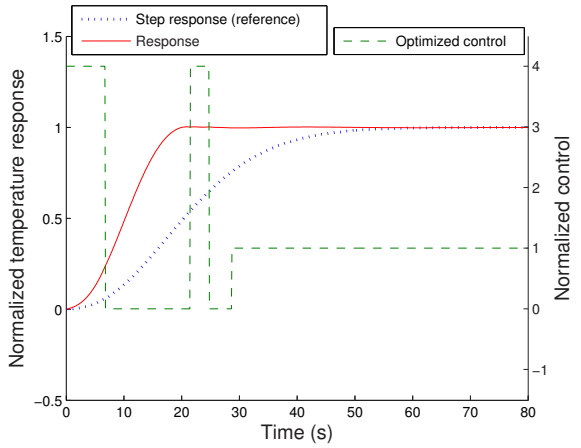


(a) Case A

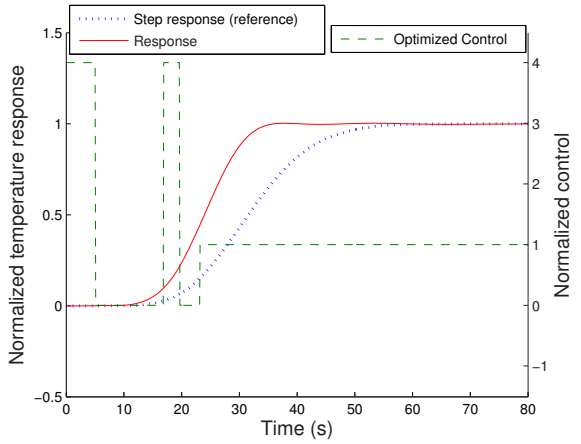


(b) Case B

5: Optimized control with method 2

optimized. The optimizer also computes the time when the control is set to its final value. The constraints on $y$, as well as the objective function, are kept from problem (13). It seems clear that this problem has a solution for any N: shortening enough the pulses durations will generate a response close to the step response which satisfies the constraints.

We denote $t_i$ the successive rise and fall times of the pulses, we choose $N = 2$ (i.e. $i = 0..4$ with $t_0 = 0$ and $t_4$ representing the time of final step change) and $u_{max} = 4$. The problem is formulated as

$$\min_{(t_1,\ldots,t_N)} \int_0^H (y^c - y(\tau))^2 d\tau$$

$$\begin{cases} t_i & \leq & t_{i+1} & \leq H & \forall i \in \{1,\ldots,2N-1\} \\ y(t) & \leq & y^c + \varepsilon & & \forall t \in [0,H] \\ y(t) & \geq & y^c - \varepsilon & & \forall t \in [T,H] \end{cases} \tag{14}$$

In the same way as in subsection IV-A the response can be quickly evaluated by

$$y(t) = u_{max} \sum_{i=0}^{N-1} (g(t - t_{2i}) - g(t - t_{2i+1})) + g(t - t_N)$$

Case A

| Method | Rise time (s) | Energy expense index | Computational effort index |
|---|---|---|---|
| Inversion | 19.77 | 86.18 | 12.53 |
| Optimization 1 | 19.70 | 71.73 | 18.54 |
| Optimization 2 | 19.74 | 71.73 | 1.000 |

Case B

| Method | Rise time (s) | Energy expense index | Computational effort index |
|---|---|---|---|
| Inversion | 35.40 | 2.19 $10^6$ | 4881 |
| Optimization 1 | 34.28 | 68.59 | 42.93 |
| Optimization 2 | 35.30 | 68.93 | 1.000 |

I: Performance & Cost

Results of optimizations for cases A and B are presented in Fig. (5). Control is simpler and time duration after which the control has reached its final value has been reduced. As shown in Table I performance in terms of output variation has remained very close to the previous case. Moreover, the number of variables in the optimization problem has been considerably reduced, allowing a substantial reduction of the computational effort.

### C. Inversion of the Resulting Trajectory

We can notice that the trajectory resulting from optimization in Section IV "takes off" much slower than the trajectory used for inverse control in Section III. We can wonder if the "shaking" inverse control is caused by a wrongly chosen trajectory. In order to check this point we inverse the trajectory obtained with optimization in Section IV. Fig. (6) presents the inversion-based control corresponding to the trajectory obtained in Fig. (5a). We notice close matching between the two controls despite inaccuracy which is certainly due to difficulties in evaluating (12). This logically points out the fact that the trajectory should not be chosen as a simple transition function.

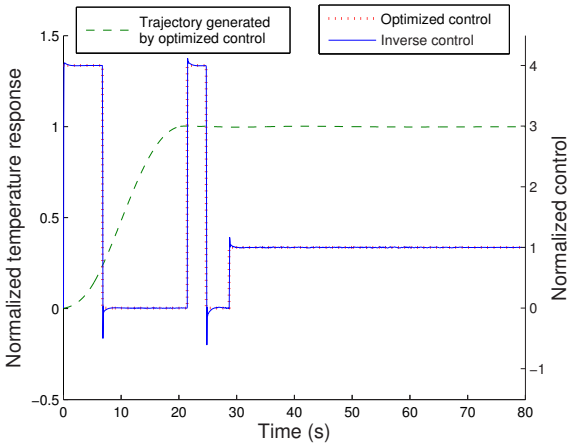


6: Inverse control for optimized trajectory - case A

## V. CONCLUSIONS AND FUTURE WORKS

### A. Conclusions

In this paper, we presented a distributed parameter model which, despite numerous simplifying assumptions, is in great accordance with experimental data obtained on Diesel Oxidation Catalyst (DOC) test bench. Formally, we have shown how the derived input-output transfer function, which involves delays and Bessel function among others, could be inverted, yielding a straightforward solution to the motion planning problem. Based on scenarios of engineering interest, we stressed that this simple strategy has some serious shortcomings. It seems that output histories (here represented by a classic Gevrey function) require a design method, which is likely to come from mathematical analysis, to prevent the high frequencies and large amplitude jumps observed on corresponding input values. Fortunately, these "jumps" are not necessary and are, in facts, useless. Interestingly, the general shape of the obtained signal is insightful, and can serve as an initial guess for numerical methods which can deal with explicit constraints. We presented two such methods, which, as it is demonstrated, are simple to implement and produce efficient solutions.

Our current research focuses on improving the discussed methods. We desire to get more insight into the formal computations and determine which family of functions is appropriate as inputs to the inverse problem. On the other hand, the numerical method can be improved and generalized to incorporate further neglected details, which in some situations, could be important.

### B. Future Works

In all our results, we notice that a very good mean to accelerate the system is to use a pulsed control. That could be used as an online control method, which is the subject of on-going works. Of course, we also consider the practical case of reductants oxidation -i.e. spatially distributed heat generation-, that will be the subject of forthcoming publications.

## VI. APPENDIX

### A. Inverse Laplace transform of $\hat{T}$

Let $\delta(t)$ denote the Dirac function and $*$ the convolution. Using inverse Laplace transform [10] [11] we get

$$\begin{aligned}
&\mathcal{L}^{-1}\left(\hat{T}(z,s)\exp\left(\frac{z}{v}s+\frac{k_1 z}{v}\right)\right)\\
&=\mathcal{L}^{-1}\left(\hat{u}(s)\exp\left(\frac{m}{s+k_2}\right)\right)\\
&=\left(\exp\left(-k_2 t\right)\mathcal{L}^{-1}\left(\exp\left(\frac{m}{s}\right)\right)\right)*\mathcal{L}^{-1}\left(\hat{u}(s)\right)\\
&=\left(\exp\left(-k_2 t\right)\left(\delta(t)+\sqrt{\frac{m}{t}}I_1(2\sqrt{mt})\right)\right)*u(t)\\
&=\left(\exp\left(-k_2 t\right)\delta(t)\right)*u(t)+e^{-k_2 t}\sqrt{\frac{m}{t}}I_1(2\sqrt{mt})*u(t)\\
&=u(t)+\int_0^t e^{-k_2\tau}\sqrt{\frac{m}{\tau}}I_1(2\sqrt{m\tau})u(t-\tau)d\tau
\end{aligned}$$

So,

$$\begin{aligned}
T(z,t)=\Upsilon(t-\frac{z}{v})\exp\left(-\frac{k_1 z}{v}\right)\times\Bigg[u(t-\frac{z}{v})+\dots\\
\dots\int_0^{t-z/v}\exp\left(-k_2\tau\right)\sqrt{\frac{m}{\tau}}I_1(2\sqrt{m\tau})u(t-\frac{z}{v}-\tau)d\tau\Bigg]
\end{aligned}$$

### B. Series expansion of an integral term

Noting $w=2\sqrt{m\tau}$, $dw=\sqrt{m/\tau}d\tau$ and $b=k_2/(4m)$, integral representation in (8)

$$\int_0^{t-z/v}\exp\left(-k_2\tau\right)\sqrt{\frac{m}{\tau}}I_1(2\sqrt{m\tau})d\tau \tag{15}$$

can be transformed into

$$\int_0^{2\sqrt{m(t-z/v)}}\exp(-bw^2)I_1(w)dw. \tag{16}$$

Provided the following result [12]

$$\int_0^t\exp(-mv^b)v^{\alpha-1}dv=\frac{m^{-\alpha/b}}{b}\Gamma(\alpha/b)\Gamma_{\text{inc}}(mt^b,\alpha/b), \tag{17}$$

where

$$\Gamma_{\text{inc}}(x,m)=\frac{1}{\Gamma(m)}\int_0^x t^{m-1}\exp(-t)dt$$

and because the Bessel function $I_1$ [10] can be represented with

$$I_1(x)=\sum_{r=0}^{\infty}\frac{1}{r!(r+1)!}\left(\frac{x}{2}\right)^{2r+1} \tag{18}$$

it is possible to write the integral (15) as an infinite sum of standard functions: we can use the series decomposition (18) in integral (16), and use the property (17). Finally, this yields

$$\begin{aligned}
&\int_0^{t-z/v}\exp(-k_2\tau)\sqrt{\frac{m}{\tau}}I_1(2\sqrt{m\tau})d\tau\\
&=\textstyle\sum_{r=1}^{\infty}\dfrac{\Gamma_{\text{inc}}(k_2(t-z/v),r)}{r!(k_2/m)^r}.
\end{aligned}$$

### C. Inverse Laplace transform of $\hat{u}$

$$\begin{aligned}
&\mathcal{L}^{-1}\left(\hat{u}(s)\exp\left(-\frac{k_1 z}{v}\right)\right)\\
&=\mathcal{L}^{-1}\left(\exp\left(-\frac{m}{s+k_2}\right)\hat{F}(s)\right)\\
&=\left(\exp\left(-k_2 t\right)\mathcal{L}^{-1}\left(\exp\left(-\frac{m}{s}\right)\right)\right)*\mathcal{L}^{-1}\left(\hat{F}(s)\right)\\
&=\left(\exp\left(-k_2 t\right)\left(\delta(t)-\sqrt{\frac{m}{t}}J_1(2\sqrt{mt})\right)\right)*f(t)\\
&=\left(\exp\left(-k_2 t\right)\delta(t)\right)*f(t)-\dots\\
&\quad\dots\left(\exp\left(-k_2 t\right)\sqrt{m/t}J_1(2\sqrt{mt})\right)*f(t)
\end{aligned}$$

We finally get

$$\begin{aligned}
u(t)=\exp\left(\frac{k_1 z}{v}\right)\Upsilon(t)\Bigg[f(t)-\dots\\
\dots\int_0^t\sqrt{\frac{m}{\tau}}J_1(2\sqrt{m\tau})\exp\left(-k_2\tau\right)f(t-\tau)d\tau\Bigg]
\end{aligned}$$

## REFERENCES


[1] AECC website, Sept. 2007, Available: http://www.aecc.eu/

[2] E.J. Bisset, Mathematical model of the thermal regeneration of a wall-flow monolith Diesel particulate filter, *Chem. Eng. Sci.*, vol. 39, 1984, pp 1232-1244.

[3] L. Achour, Dynamique et contrôle de la régénération d'un filtre à particules Diesel, PhD Thesis, École des Mines de Paris, 2001

[4] S.H. Oh, J.C. Cavendish, Transients of monolithic catalytic converters: response to step changes in feedstream temperature as related to controlling automobile emissions, *Ind. Eng. Chem.*, vol. 21, 1982, pp 29-37.

[5] G.C. Koltsakis, A.M. Stamatelos, Catalytic automotive exhaust aftertreatment, *Prog. Energy Combust. Sci.*, vol. 23, 1997, pp 1-39.

[6] C. Depcik, D. Assanis, One-dimensional automotive catalyst modeling, *Prog. Energy Combust. Sci.*, vol. 31, 2005, pp 308-369.

[7] J. Vardi, W.F. Biller, Thermal behavior of an exhaust gas catalytic converter, *Ind. Eng. Chem.-Process Des. Dev.*, vol. 7, 1968, pp 83-90.

[8] M.N. Osizik, Basic heat transfer, McGraw-Hill, Feb. 1977.

[9] B. Laroche, P. Martin, P. Rouchon, Motion planning for the heat equation, *Int. J. Rob. Nonlinear Control*, 2000.

[10] M. Abramowitz, I. A. Stegun, Handbook of mathematical functions, Dover Publications, June 1965

[11] A. Angot, Compléments de mathématiques à l'usage des ingénieurs de l'électrotechnique et des télécommunications, 6ème éd., Masson, 1982.

[12] Wolfram Research, Inc., The Wolfram functions site, Dec. 2006, Available: http://functions.wolfram.com/